Environ. Sci. Technol. **2005**, *39,* 5227−5233

Link between Chemotactic Response to Ni^{2+} and its Adsorption onto the *Escherichia coli* Cell Surface

DAVID BORROK,*,† M. JACK BORROK,‡ JEREMY B. FEIN,† AND LAURA L. KIESSLING‡,§

Department of Civil Engineering and Geological Sciences, University of Notre Dame, Notre Dame, Indiana 46556, andDepartments of Biochemistry and Chemistry, University of Wisconsin, Madison, Wisconsin 53706

Bacterial chemotaxis is of medical, biological, and geological significance. Despite its importance, current chemotaxis measurements fail to account for the speciation of the chemical effector and the protonation state of the bacterial surface. We hypothesize that adsorption of Ni^{2+} onto the surface of *Escherichia coli* can influence its effective concentration and therefore influence its ability to induce a repellent response. By measuring repellent response at different pH values, the influence of Ni^{2+} adsorption on chemotaxis was assessed. In addition, we tested the effect of different Ni^{2+} chelating agents. Our data indicate that adsorption reactions influence the chemotactic response to Ni^{2+}. We use potentiometric titration and Ni^{2+} adsorption experiments to develop and constrain a thermodynamic model capable of quantifying the concentration of Ni^{2+} at the bacteria/solution interface. Results from this model predict that the concentration of adsorbed Ni^{2+} is linearly proportional to the magnitude of the chemotactic response in *E. coli*. If adsorption is linked to chemotaxis in other cases, then chemotactic responses in realistic settings depend on a number of environmental factors such as pH, competing binding agents (e.g., aqueous organic acids, natural organic matter, mineral surfaces, etc.), and ionic strength. Our modeling approach quantifies adsorbed species on bacterial surfaces and may be used to predict the responses of different species to a variety of chemoeffectors. Our data suggest that specified changes in environmental conditions can be used to tune chemotactic responses in natural biological and geological settings.

Introduction

Motile bacteria utilize specialized sets of protein receptors in their cell membranes to sense and respond to minute chemical gradients in their environments through chemotaxis (*1*). Signals sent from chemoreceptors regulate flagella rotation, which in turn propels the bacteria toward attractants or away from repellents (*2*−*6*). Bacterial chemotaxis is linked to microbial pathogenesis (*7*) and can play a critical role in the cycling and remediation of chemicals in geologic settings (*8*−*13*). Different organic and inorganic chemicals have been shown to induce chemotactic responses in a range of bacterial species (*14*, *15*), and many models have been developed for quantifying the migration of motile bacteria in response to chemical stimulants (*16*−*18*). The extrapolation of these observations and models from laboratory systems to realistic settings, however, is problematic.

The pH values of biological and geological environments can vary substantially, ranging from pH < 3.0 in acid mine drainage settings (*19*) to pH > 8.0 in ocean and freshwater carbonate systems. Moreover, many competing binding agents that can significantly affect speciation of both the aqueous chemical effector and the bacterial surface are found in the natural settings. In addition to the limited number of chemosensing proteins, bacterial cell surfaces contain high concentrations of organic acid functional groups that can bind aqueous metal cations (*20*, *21*), as well as hydrophobic and ionizable organic compounds (*22*). Solution pH controls the protonation state of these functional groups and thereby the bacterial surface charge. Thus, pH can influence surface adsorption reactions that impact the chemical environment at the bacterial surface. Because environmental factors such as pH can greatly change the affinity of some chemoeffectors, especially anionic or cationic species, for the bacterial surface, we postulated that these environmental factors can influence the chemotactic response. If such a model is valid, it is not the concentration of a stimulant in bulk solution but rather its concentration at the bacteria/solution interface that determines bacterial chemotactic response. Hence, model predictions of chemotactic movement toward or away from effectors that can interact with the bacterial cell surface must account for these factors. To date, chemotaxis experiments have not measured the effects of cell surface or effector speciation on chemotactic response.

In this study, we test the hypothesis that adsorption of chemoeffectors to the bacterial cell surface can influence chemotactic responses. To this end, we examined chemorepulsion to Ni^{2+} in *Escherichia coli* under different conditions. We conducted experiments in which the total concentration of Ni^{2+} in solution is held constant, but the pH or the concentration of a competing Ni^{2+} chelating agent (ethylenediaminetetraacetic acid, EDTA) is varied. Parameters such as pH or binding agents (the concentration of EDTA) are illustrative of the types of variables that can change in different geologic settings. We also conduct potentiometric titration and Ni^{2+} adsorption experiments using *E. coli*. These data were used to develop a thermodynamic model capable of predicting chemotactic responses in multicomponent systems by quantifying the concentration of the stimulant at the bacterial surface.

Materials and Methods

Culture Methods. The *E. coli* K-12 (AW607) strain used in chemotaxis experiments was grown at 30 °C in 100 mL of Luria broth (LB) medium for approximately 4 h, reaching an optical density of 0.2−0.3 (∼0.5 wet g/L), as measured at a wavelength of 600 nm. Cells used for titration and adsorption experiments were grown at 30 °C in 1 L of LB medium for 20 h. Cells were harvested and washed three times in 3 mM $NaClO_4$ (the same electrolyte used in all experiments), and the wet weight of the cells was determined (*23*, *24*).

Two-Dimensional Motion Analysis. A Nikkon E800 microscope with a 60× objective was used to examine the chemotactic response of *E. coli* to aqueous Ni^{2+} at different

* Corresponding author phone: (574) 631-4307; fax: (574) 631-9236; e-mail: dborrok@nd.edu.
† University of Notre Dame.
‡ Department of Biochemistry, University of Wisconsin.
§ Department of Chemistry, University of Wisconsin.

10.1021/es0482381 CCC: $30.25
Published on Web 06/15/2005

pH values or in the presence of different concentrations of EDTA. Bacteria, suspended in a stock solution of 3 mM $NaClO_4$, were exposed to various pH values (by addition of small amounts of NaOH or HCl) or EDTA concentrations. *E. coli* were given 2 min to adjust to changes in pH or EDTA concentration prior to measurement. A pH-neutralized, concentrated $NiSO_4$ solution was added to a final concentration of 100 μM, and the bacteria were immediately placed on the stage. These additions did not significantly impact solution pH. A motion analysis camera was used to track motile bacteria, and results were analyzed by use of Datapoint video analysis software. Similar two-dimensional motion analysis experiments have been described previously (*25*). The average angular velocity was determined by measuring changes in movement (in *x* and *y* dimensions only) for each individual bacterium from frame to frame within each video analysis (*26*). Statistical analysis was performed by averaging the angular velocities of all bacteria present within the viewing area in 18 frames taken over a 6 s time span. Experiments were conducted in the absence of Ni^{2+} to determine the effect of pH and EDTA on bacterial chemotaxis. These measurements were necessary to verify that the chemotactic behavior of *E. coli* is not affected by changes in either pH or EDTA under our experimental conditions. Additional experiments examined the chemotactic response of *E. coli* to 10 mM leucine or 100 μM maltose at various pH values (also in a 3 mM $NaClO_4$ buffer). The results from these experiments indicate that the proteins responsible for regulating the chemotactic response of *E. coli* function properly over the entire pH range of our experiments.

Potentiometric Titration and Nickel Adsorption Experiments. For titration experiments, cells washed three times in 3 mM $NaClO_4$ buffer were suspended in approximately 10 mL of 3 mM $NaClO_4$ that had been purged of CO_2 by sparging with N_2 for 60 min. The suspension was immediately placed into a sealed titration vessel maintained under a positive pressure of N_2. Titrations were conducted in triplicate by use of an automated buret assembly. Each suspension was first titrated to the desired starting pH of approximately 2.7, using minute aliquots of 1.040 N HNO_3. Forward titrations were then performed to an approximate final pH of 9.5 through the addition of aliquots of 1.028 N NaOH. The pH of each bacterial suspension was monitored so that each aliquot of titrant was added only after the pH of the suspension became stable at 0.001 pH unit/s. Stabilization of the pH after each addition of titrant generally occurred in less than 60 s. The total volume of acid or base added during each titration ranged from about 2.5% to 3.5% of the starting volume of the solution, and the starting concentration of bacteria in each suspension was ~65 wet g/L for all titrations. The change in ionic strength over the course of the titration was ~1 mM. Previous studies suggest that minor changes in ionic strength have a negligible effect on titration results (*27*, *28*).

Ni^{2+} adsorption experiments were conducted following procedures similar to those of batch metal adsorption experiments described previously (*23*, *24*, *29*), with 5 or 0.5 g/L *E. coli* cells. The cells were suspended in a pH-neutralized stock solution of 100 μM Ni^{2+} and 3 mM $NaClO_4$. The stock solution was divided into individual reaction vessels, and the pH of each vessel was adjusted by adding minute aliquots of 1.0 or 0.1 M HNO_3 or NaOH. After adjustment of the pH and an additional 2 h of reaction time on a rotating rack, the final (equilibrium) pH of each vessel was measured. The individual vessels were then centrifuged and the resultant supernatant was filtered through a 0.45 μm nylon membrane. The filtered supernatant was analyzed for Ni^{2+} with a Perkin-Elmer Optima 2000 inductively coupled plasma−optical emission spectrometer, using matrix-matched standards. Analytical error was determined to be less than ±2%. The amount of Ni^{2+} adsorbed to the bacterial surface was calculated by difference (total $[Ni^{2+}]$ − supernatant $[Ni^{2+}]$). Previous experiments in our laboratory show that adsorption onto the experimental apparatus is negligible and that metal adsorption to the cellular surface is a fully reversible equilibrium process (i.e., no measurable cellular uptake of metal; *30*).

Results and Discussion

Ni^{2+} Chemotaxis Experiments. We used motion analysis to examine the repellent response to Ni^{2+} in *E. coli* under different environmental conditions. The periplasmic Ni^{2+} binding protein (NikA) of *E. coli*, which is involved in chemotaxis, has been widely studied (*31*, *32*); the structure of this protein has recently been determined by X-ray crystallographic analysis (*33*). Repellents such as Ni^{2+} induce an increase in tumbling frequency, which corresponds to an increase in the average angular velocity of individual bacterial cells over short periods of time (~6 s). The cellular envelope of *E. coli* also contains organic acid functional groups that become deprotonated as pH increases. Thus, more anionic sites are available to adsorb Ni^{2+} in basic environments. We hypothesized that greater adsorption should increase the effective concentration of Ni^{2+} at the bacterial surface, heightening repellent response.

To test our hypothesis, we first evaluated the chemotactic response of *E. coli* to 100 μM Ni^{2+} at a variety of pH values. We found that as we increased the pH above 5.5, the average angular velocity (tumbling frequency) for *E. coli* steadily increased. A maximum angular velocity of 57 deg/frame is obtained at pH 8.4 (the highest pH tested, Figure 1A). Aqueous Ni^{2+} did not precipitate nor appreciably hydrolyze [e.g., $Ni(OH)^+$, $Ni(OH)_2^0$, etc.] over the range of pH values used in our experiments (*34*). To assess whether changes in pH alone influence angular velocity, experiments with no Ni^{2+} were performed. The motion of *E. coli* was monitored in Ni-free samples over the pH range of 4.5−8.4, and no significant changes in *E. coli* chemotaxis were observed (Figure 1A). These results indicate that the measured chemotactic response to Ni^{2+} is not caused by changes in solution pH. The background average angular velocity established in these experiments represents the minimum average angular velocity expected in the experimental system with no chemical stimulant. The background is greater than zero due to random changes in swimming direction and physical forces such as Brownian motion. Similar procedures and background values have been established in previous studies (e.g., ref *25*). Together, our data suggest that the observed increase in repellent response at higher pH values is due to a higher effective concentration of Ni^{2+} at the cell surface.

We also tested the ability of a soluble Ni^{2+} binding agent (EDTA) to manipulate the concentration of the repellent at the bacterial surface and therefore influence chemotactic response. When the pH (6.7) and total nickel concentration (100 μM) in solution were held constant, the average angular velocity of *E. coli* decreased as a function of increasing EDTA concentration (Figure 1B). The average angular velocity is 48 ± 6 deg/frame when EDTA is absent and decreases to a minimum of 24 ± 3 deg/frame in the presence of 75 μM EDTA. No significant change in the average angular velocity for *E. coli* was observed when 100 μM EDTA alone was added (Figure 1B). These data indicate that the repellent activity of Ni^{2+} is diminished in the presence of the metal chelator EDTA. Thus the effects of EDTA on bacterial chemotaxis are presumably due solely to its ability to sequester Ni^{2+}.

We attribute the observed behavior in both experiments to changes in the concentration of Ni^{2+} at the bacteria cell surface/solution interface. Ni^{2+} readily forms complexes with the negatively charged carboxyl, phosphoryl, and hydroxyl functional groups present on the *E. coli* surface (*35*). As these functional groups undergo deprotonation at increasing pH

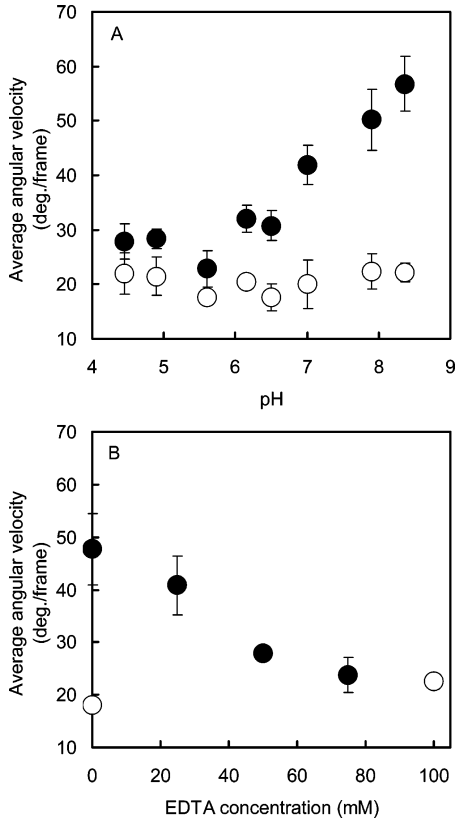

FIGURE 1. Negative chemotaxis of *E. coli* cells in response to Ni^{2+}. (A) Angular velocity measured as a function of pH at constant (100 μM) aqueous Ni^{2+} concentration (●) or with no Ni^{2+} present (○). (B) Angular velocity measured as a function of aqueous EDTA concentration at constant (100 μM) Ni^{2+} concentration (●) and control measurement with no Ni^{2+} present (○). Error bars in both panels are 2σ uncertainties based on averages of three or more 6 s videos (minimum 15 individual bacterial paths were measured per data point).

values, more Ni^{2+} becomes adsorbed to the anionic sites on the bacterial cell envelope. Thus, the repellent response is heightened at higher pH values where more Ni^{2+} is adsorbed to the bacterial surface. Similarly, as EDTA is added to solution, aqueous Ni^{2+}−EDTA complexes become more abundant; less Ni^{2+} is concentrated at the bacterial cell surface. These results suggest that the bacterial chemotactic response cannot always be predicted by measuring the concentration of a repellent or attractant in bulk solution. Models to estimate the concentration of the effector chemical at the bacteria/solution interface are needed to more accurately predict microbial behavior.

***E. coli* Responses to Leucine and Maltose.** Our results suggest that chemotactic responses to Ni^{2+} are influenced by the adsorption of Ni^{2+} to the bacterial surface, and this adsorption is influenced by pH. An alternate interpretation of these results is that changes in pH influence the chemotactic machinery in *E. coli* by ionizing specific chemoreceptors that interact with Ni^{2+}. To explore this alternative explanation, chemotactic responses to the repellent leucine and the attractant maltose were measured. These chemoeffectors were chosen because they are nonpolar organic compounds that should not change their speciation or degree of hydrophobicity appreciably over the pH range studied. Therefore, unlike Ni^{2+}, the concentrations of these compounds at the bacteria/solution interface are not expected to change appreciably as a function of pH.

As predicted, we observe little change in chemotactic response over the pH range studied. For example, the attractant response to maltose is observed at all pH values tested, as shown by a decrease in angular velocity over unstimulated cells (Figure 2). In addition, the repellent response to leucine was also maintained over the tested pH range, as shown by an increased tumbling frequency over unstimulated cells. The average angular velocities measured in all experiments (with leucine, maltose, or no stimulant present) are consistent from pH 4.5 to 7.5 but increase slightly at pH 8.9 (Figure 2). Because all of the average angular velocities increase proportionally at pH 8.9, this behavior represents an increase in the background level of the average angular velocity of the system and not a change in the chemosensing machinery of *E. coli*. This increase in average angular velocity might be a mild chemotactic response or an alteration in swimming behavior caused by disruption of the cell membrane at high pH. This behavior was not detected in experiments in the Ni^{2+}−*E. coli* experimental system; we found that that the background average angular velocity remains constant to pH 8.4 (Figure 1A).

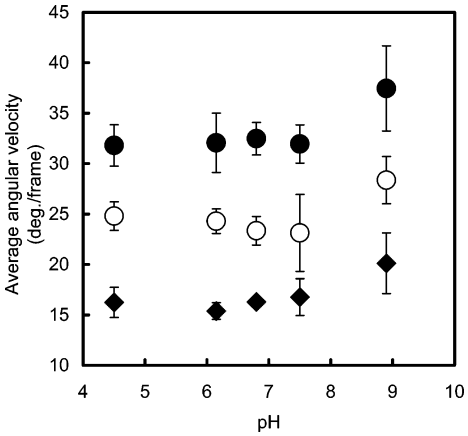

FIGURE 2. Chemotaxis of *E. coli* cells in response to leucine and maltose. Angular velocity is measured as a function of pH at constant (10 mM) leucine (●) and (100 μM) maltose (◆) concentrations. Control measurements with no stimulant present were also performed (○). Error bars are 2σ uncertainties based on averages of three or more 6 s videos.

These results indicate that the chemotactic responses of *E. coli* to both leucine and maltose are relatively insensitive to pH. Both the maltose−maltose binding protein complex and the Ni^{2+}−NikA binding complex interact with the Tar chemoreceptor to transmit signals to the cytoplasmic chemotaxis components. Because changes in pH had little influence on chemotaxis to maltose, the Tar chemoreceptor signaling pathway in *E. coli* is not appreciably affected by pH changes over the range studied. To evaluate whether changes in NikA binding to Ni^{2+} are expected to be sensitive to pH, we examined the structure for NikA determined by X-ray crystallography (*33*). No ionizable functional groups are involved in hydrogen bonding to the five water molecules that coordinate aqueous Ni^{2+}. Similarly, the predicted NikA−Tar interface has no groups that would be expected to undergo changes in ionization over the pH range studied. We conclude from our data and these analyses that the changes in cellular response to Ni^{2+} as a function of pH (Figure 1A) are not due to changes in the ionization of the NikA binding protein or to changes in occupied NikA binding to Tar.

Modeling, Potentiometric Titration, and Ni^{2+} Adsorption Experiments. Surface complexation models can be used to successfully predict the concentrations of adsorbed metals and organic molecules on bacterial surfaces in multicomponent systems (*22*−*24*, *29*, *36*). We use this chemical equilibrium modeling approach to explicitly account for the

TABLE 1. Proton and Ni^{2+} Binding Stability Constants and Functional Group Site Concentrations for *E. coli*[a]

discrete functional group site	proton binding stability constants and 1σ uncertainties (pK_a)	avg site concns and 1σ uncertainties ($\times 10^{-5}$ mol/wet g)	Ni^{2+} binding stability constants (log *K*)
1	3.3 ± 0.1	8.1 ± 0.2	3.1 ± 0.2
2	5.2 ± 0.1	7.6 ± 1.2	3.7 ± 0.2
3	6.8 ± 0.1	4.8 ± 0.2	2.6 ± 0.2
4	9.0 ± 0.1	4.7 ± 0.5	5.9 ± 0.2

[a] Parameters were calculated through modeling of titration and adsorption experiments performed at a starting ionic strength of 0.003 M. Proton and Ni^{2+} stability constants are defined as follows: $K_a = ([R\text{-}A^-]a_{H^+})/([R\text{-}AH^0])$ and $K = ([R\text{-}A(Ni)^+])/(a_{Ni^{2+}}[R\text{-}A^-])$, with the individual components in each equation defined in the text. Uncertainties (1σ) are based on triplicate titrations for proton stability constants and site concentrations and are estimated by a data fitting procedure for Ni^{2+} stability constants.

complexation of protons and Ni^{2+} with the functional groups present on the cell surface of *E. coli*. Experimental data were employed to calculate equilibrium constants and/or concentrations of individual chemical species in each experimental system. We represent functional groups present on the surface of *E. coli* using a number of discrete monoprotic acids, each of which undergoes deprotonation. Ni^{2+} complexation with the deprotonated forms of a monoprotic acid can be expressed as

$$Ni^{2+} + [R\text{-}A^-] \leftrightarrow [R\text{-}A(Ni)^+] \quad (1)$$

with an equilibrium constant, *K*, for this reaction given by

$$K = \frac{[R\text{-}A(Ni)^+]}{a_{Ni^{2+}}[R\text{-}A^-]} \quad (2)$$

where R is the bacterium to which the functional group type, A, is attached, $[R\text{-}A^-]$ is the concentration of deprotonated sites, $[R\text{-}A(Ni)^+]$ is the concentration of the Ni^{2+} functional group site complex, and $a_{Ni^{2+}}$ is the aqueous activity of the metal cation. For this modeling application, we assume a 1:1 stoichiometric ratio for Ni^{2+} binding to each deprotonated ligand. Although this stoichiometric ratio is shown to be valid under the experimental conditions studied here, further testing would be necessary to ensure that the hypothesized stoichiometric ratio is valid (and remains the same) under different conditions, particularly those where bacterial surface site saturation may occur.

Titrations of *E. coli* suspensions were performed in triplicate under conditions in which the ionic strength was adjusted to match (as closely as possible) those of the chemotaxis experiments (Figure 3). The data indicate that *E. coli* cells possess significant buffering capacity over the entire pH range of interest (~3−9). The number of discrete functional group sites on the bacterial surface, the concentrations of each site, and the corresponding stability constants for each site were determined through modeling of this potentiometeric titration data (Table 1). Modeling parameters were calculated with the chemical equilibrium program FITEQL 2.0 (*37*). We neglected the effects of the surface electric field on the adsorption reactions (nonelectrostatic model) because all of the experiments were conducted at a single ionic strength value (0.003 M). Activity coefficient calculations were performed within FITEQL by use of the Davies equation. We determine the minimum number of discrete functional group types that are required to account for the observed buffering capacity by sequentially testing models with one through five proton-active sites. For each titration data set, a four-discrete-site model yielded significantly better fits than models with fewer sites, and the data could not constrain

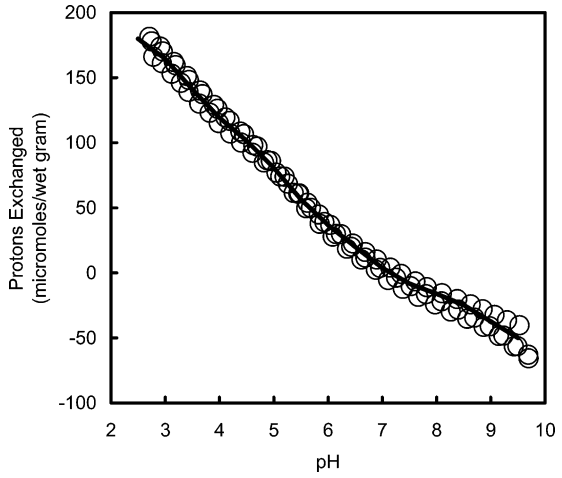

FIGURE 3. Raw data for triplicate potentiometric titrations of *E. coli* cells. Experiments were conducted at a starting ionic strength of 0.003 M ($NaClO_4$), with a bacterial concentration of ~65 wet g/L. The averaged model fit for all the titration data is presented as a solid curve.

models with five or more sites. The goodness of each fit was determined by use of the variance function, $V(Y)$, within the FITEQL program (*37*). The concentration of each site and the stability constant for each deprotonation reaction ($[R\text{-}AH^0] \leftrightarrow [R\text{-}A^-] + H^+$) was also determined through modeling of the titration data. The average pK_a (−log K) values for the four deprotonation reactions are 3.3, 5.2, 6.8, and 9.0 (Table 1), and the average model fit (based on these parameters) is presented with the raw titration data in Figure 3.

The functional group site concentrations and pK_a values were used in conjunction with the experimental measurements of Ni^{2+} adsorption onto *E. coli* cells to calculate Ni^{2+}−bacterial surface stability constants, as described by Fein et al. (*29*). Using FITEQL, we tested Ni^{2+} adsorption onto the bacterial surfaces modeled as a reaction between Ni^{2+} and a deprotonated surface site (adsorption onto each discrete site, both individually and in combination, was tested in each case) to form a bacterial surface complex (see eq 2). Ni^{2+} stability constants could not be calculated for the discrete sites with deprotonation constants of 3.3 and 5.2 by use of the adsorption data collected at a low concentration of bacteria (0.5 g/L). Negligible concentrations of Ni^{2+} were adsorbed in this experiment under the low-pH conditions where these sites become deprotonated. To avoid this problem, we used the adsorption data collected from a higher concentration of bacteria (5.0 g/L) to calculate Ni^{2+} stability constants. Adsorption of Ni^{2+} to all four deprotonated sites was necessary to account for the observed adsorption behavior. Ni^{2+} stability constant values for the four discrete sites with pK_a values of 3.3, 5.2, 6.8, and 9.0 are 3.1, 3.7, 2.5, and 5.9, respectively (Table 1). Both the 0.5 and 5.0 g/L Ni^{2+} adsorption data are presented in Figure 4 along with the corresponding model fits. The model fits are produced from FITEQL to generate a curve based entirely on the experimental conditions (i.e., 5 or 0.5 g/L bacteria and 100 μM Ni^{2+}) and the proton and Ni^{2+} stability constants presented in Table 1. Hence, the Ni^{2+} stability constants that were developed from the 5.0 g/L data set were also used to model the 0.5 g/L data (Figure 4). The predicted extent of adsorption for the 0.5 g/L system is in good agreement with the measured extent of adsorption, providing additional support for the validity and robust nature of the stability constant values derived in our study.

Relating Adsorption and Chemotaxis. We use the newly developed *E. coli* modeling parameters in conjunction with published EDTA deprotonation and Ni^{2+} binding constants

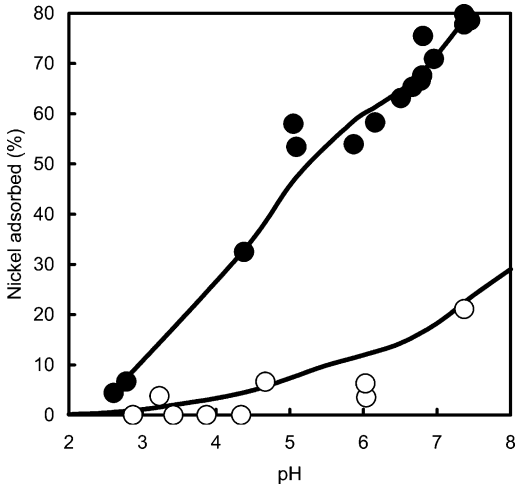

FIGURE 4. Ni^{2+} adsorption onto *E. coli* cells as a function of pH. Adsorption data are for 5 g/L (●) and 0.5 g/L (○) *E. coli* at 100 μM Ni^{2+}. The fit for the 5 g/L data (solid curve) is the best fit based on modeling of the 5 g/L data, while the model fit for the 0.5 g/L data (solid curve) is an independent model prediction made by use of the modeling constants developed from the 5 g/L model. Both model fits are based on a four-discrete-site surface complexation model with Ni^{2+} binding onto each of the four deprotonated surface sites.

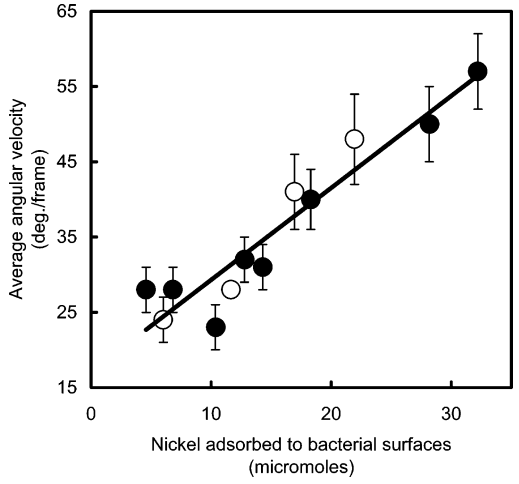

FIGURE 5. Negative chemotaxis as a function of the concentration of Ni^{2+} adsorbed to the surface of *E. coli*. Angular velocity was measured previously as a function of pH (●) and EDTA (○) concentration (Figure 1). Error bars are 2σ uncertainties based on averages of three or more 6 s videos. The concentration of Ni^{2+} bound to *E. coli* was calculated by use of a surface complexation model that accounts for the effects of pH and EDTA concentrations on bacteria and nickel speciation.

(*38*) to determine the concentration of Ni^{2+} adsorbed to the bacterial surface at every pH value and EDTA concentration. The concentration of Ni^{2+} adsorbed is a proxy for the amount of Ni^{2+} at the bacterial surface/solution interface. A linear correlation between the observed chemotactic response of the bacteria and the calculated concentration of adsorbed Ni^{2+} on the *E. coli* cell surface was obtained, with a linear correlation coefficient of 0.91 (Figure 5). This linear correlation is obtained for experiments in which the concentration of cell-surface-adsorbed Ni^{2+} is controlled by pH effects and those in which EDTA competes with the cell-surface Ni^{2+}. These results strongly suggest that surface adsorption of Ni^{2+} is a controlling factor in the chemotactic response of *E. coli* to this chemorepellent. However, the exact mechanism whereby adsorbed Ni^{2+} on the bacterial envelope is sensed by the periplasmic Ni^{2+} binding proteins responsible for chemotaxis remains uncertain. The role of adsorption in chemotaxis has been overlooked in previous studies because the majority of chemotaxis experiments are performed in a buffered solution at a constant pH value (for example, refs *11*, *14*, and *15*). Moreover, the importance of adsorption depends on the type of attractant or repellent under study as well as the environmental conditions.

Using the modeling approach developed in this study to determine the concentration of cell-adsorbed Ni^{2+} and relationship of adsorbed Ni^{2+} to chemotactic response, we can successfully predict the chemotactic response of *E. coli* to Ni^{2+} in any multicomponent system of interest for which the appropriate equilibrium constants and concentrations of Ni^{2+}-binding agents are known. For example, the chemotactic response of *E. coli* to Ni^{2+} in near-surface geologic systems containing high concentrations of dissolved natural organic matter could be calculated with the relationship depicted in Figure 5 if the concentrations and Ni^{2+}-binding capabilities of the dissolved macromolecules were known. This modeling approach can also be adopted to describe nonmetal interactions, such as those between hydrophobic or ionizable organic compounds and the bacterial cell surface (*22*, *39*).

Chemotaxis in Natural Settings. Ni^{2+} adsorption reactions on the surface of *E. coli* play a dramatic role in regulating chemotactic response by altering the effective concentration of Ni^{2+} at the bacteria/solution interface. The amplified local concentration of Ni^{2+} is then interpreted by the chemoeffector sensing machinery. Therefore, the chemotactic response of *E. coli* to Ni^{2+} under standard laboratory conditions and in a natural setting may differ. In nature, the pH and/or solution composition often differs significantly from those used in laboratory experiments. The effect of adsorption reactions on chemotaxis is likely important for other chemical effectors and other bacterial species not tested here. However, the effect is probably strongest for aqueous cationic or anionic chemoeffectors; cationic metals, perhaps, are the most likely to adsorb onto anionic functional groups on bacterial surfaces.

A significant number of bacteria possess chemoreceptors specific to metal cations (*40*, *41*). For example, it has recently been demonstrated that the facultative bacterium *Geobacter metallireducens* undergoes chemotaxis toward Fe(II) if grown on medium with insoluble Fe(III) (*8*). Our findings indicate that bacterial metal-sensing mechanisms should be most proficient at higher pH environments such as seawater and are least proficient under low-pH conditions, like acid mine drainage sites. Such a model is consistent with the ability of bacteria (and other chemotactic microorganisms) in ocean environments to successfully scavenge extremely limited metal ions. In addition to metal ions, the concentrations of some hydrophobic, polar, and ionizable organic compounds at the bacteria/solution interface vary with environmental conditions (*22*, *39*, *42*). We speculate that the chemotactic response of bacteria to some organic stimulants may also be controlled in part by adsorption reactions on the bacterial cell surface. For example, it has been shown that sorption of hydrocarbons to bacterial surfaces can inhibit the chemoreception of other chemical stimulants (*43*). One possible interpretation of this study is that adsorption of hydrocarbons changes the effective concentrations of other stimulants at the bacterial surface. However, additional testing with different chemoeffectors and bacterial species is necessary to confirm this hypothesis and to demonstrate a universal link between adsorption and bacterial chemotaxis.

Prediction of Chemotaxis in Natural Environments. To predict chemotactic responses in biologic and geologic settings, all of the important complexation reactions that involve the effector and/or the bacterial surface must be considered. The mathematical model developed in this study

is designed to account for Ni^{2+} adsorption reactions with *E. coli*; however, it provides a generalized thermodynamic framework for predicting chemotactic responses to other stimulants and for other bacterial species. If the concentrations of the individual components and the stability constants for the key complexation reactions are known, the amount of a chemical stimulant adsorbed onto any bacterial surface can be readily calculated. The magnitude of the chemotactic response of each bacterial species can be calibrated for a given chemical of interest (Figure 5). These models could then be coupled to existing bacterial transport models (*16*−*18*) to determine the overall chemotactic movement of bacteria in a given geologic environment. We speculate that it may be practical in some instances to tune chemotactic responses by manipulating the chemistry of the bacteria/solution interface without directly manipulating chemoeffectors or chemoreceptors (*44*). Changes in solution pH or in the concentration of metal-binding ligands in a system can significantly alter the bacterial surface concentration of a chemical stimulant (in this case Ni^{2+}) and thereby dramatically affect the bacterial chemotactic response to it. The approach outlined in this study provides a means for quantitative modeling of these speciation effects and their impact on bacterial chemotaxis.

Acknowledgments

We thank Professor C. Wiese (UW—Madison) for use of the Nikkon E800 microscope. Research funding was provided by the National Science Foundation through Grant EAR02-07169 and through NSF Environmental Molecular Science Institute Grant (EAR02-21966), and by National Institutes of Health Grant GM59984. D.B. was partially supported through a University of Notre Dame Arthur J. Schmitt Presidential Fellowship, and M.J.B., through a Molecular Biosciences Training Grant (GM 07215).

Literature Cited

(1) Fenchel, T. Microbial behaviour in a heterogeneous world. *Science* **2002**, *296*, 1068−1070.
(2) Bren, A.; Eisenbach, M. How signals are heard during bacterial chemotaxis: protein−protein interactions in sensory signal propagation. *J. Bacteriol.* **2000**, *182*, 6865−6873.
(3) Falke, J. J.; Hazelbauer, G. L. Transmembrane signaling in bacterial chemoreceptors. *Trends Biochem. Sci.* **2001**, *26*, 257−265.
(4) Bourret, R. B.; Stock, A. M. Molecular information processing: lessons from bacterial chemotaxis. *J. Biol. Chem.* **2002**, *277*, 9625−9628.
(5) Wadhams, G. H.; Armitage, J. P. Making sense of it all: Bacterial chemotaxis. *Nat. Rev. Mol. Cell Biol.* **2004**, *5*, 1024−1037.
(6) Szurmant, L.; Ordal, G. W. Diversity in chemotaxis mechanisms among the bacteria and archaea. *Microbiol. Mol. Biol. Rev.* **2004**, *68*, 301−319.
(7) Butler, S. M.; Camilli, A. Both chemotaxis and net motility greatly influence the infectivity of *Vibrio cholerae*. *Proc. Natl. Acad. Sci. U.S.A.* **2004**, *101*, 5018−5023.
(8) Childers, S. E.; Ciufo, S.; Lovley, D. R. *Geobacter metallireducens* accesses insoluble Fe(III) oxide by chemotaxis. *Nature* **2003**, *416*, 767−769.
(9) Pandey, G.; Jain, R. K. Bacterial chemotaxis toward environmental pollutants: role in bioremediation. *Appl. Environ. Microbiol.* **2002**, *68*, 5789−5795.
(10) Edwards, K. J.; Bond, P. L.; Banfield, J. F. Characteristics of attachment and growth of *Thiobacillus caldus* on sulphide minerals: a chemotactic response to sulphur minerals? *Environ. Microbiol.* **2000**, *2*, 324−332.
(11) Law, A. M. J.; Aitken, M. D. Bacterial chemotaxis to naphthalene desorbing from a nonaqueous liquid. *Appl. Environ. Microbiol.* **2003**, *69*, 5968−5973.
(12) Singh, P.; Cameotra, S. S. Enhancement of metal bioremediation by use of microbial surfactants. *Biochem. Biophys. Res. Commun.* **2004**, *319*, 291−297.
(13) Parales, R. E.; Haddock, J. D. Biocatalytic degredation of pollutants. *Curr. Opin. Biotechnol.* **2004**, *15*, 374−379.
(14) Seymour, F. W. K.; Doetsch, R. N. Chemotactic responses in motile bacteria. *J. Gen. Microbiol.* **1973**, *78*, 287−296.
(15) Tso, W.; Adler, J. Negative chemotaxis in *Escherichia coli*. *J. Bacteriol.* **1974**, *118*, 560−576.
(16) Keller, E. F.; Segel, L. A. Model for chemotaxis. *J. Theor. Biol.* **1971**, *30*, 225−234.
(17) Rivero, M. A.; Tranquillo, R. T.; Buettner, H. M.; Lauffenburger, D. A. Transport models for chemotactic cell populations based on individual cell behavior. *Chem. Eng. Sci.* **1989**, *44*, 2881−2897.
(18) Hillen, T. Hyperbolic models for chemosensitive movement. *Math. Models Methods Appl. Sci.* **2002**, *12*, 1007−1034.
(19) Johnson, D. B.; Hallberg, K. B. The microbiology of acidic mine waters. *Res. Microbiol.* **2003**, *154*, 466−473.
(20) Beveridge, T. J. Role of cellular design in bacterial metal accumulation and mineralization. *Annu. Rev. Microbiol.* **1989**, *43*, 147−171.
(21) Mullen, M. D.; Wolf, D. C.; Ferris, F. G.; Beveridge, T. J.; Flemming, C. A.; Bailey, G. W. Bacterial sorption of heavy metals. *Appl. Environ. Microbiol.* **1989**, *55*, 3143−3149.
(22) Daughney, C. J.; Fein, J. B. Sorption of 2,4,6-trichlorophenol by *Bacillus subtilis*. *Environ. Sci. Technol.* **1998**, *32*, 749−752.
(23) Borrok, D.; Fein, J. B.; Kulpa, C. F. Proton and Cd adsorption onto natural bacterial consortia: testing universal adsorption behavior. *Geochim. Cosmochim. Acta* **2004**, *68*, 3231−3239.
(24) Borrok, D.; Fein, J. B.; Kulpa, C. F. Cd and proton adsorption onto bacterial consortia grown from industrial wastes and contaminated geologic settings. *Environ. Sci. Technol.* **2004**, *38*, 5656−5664.
(25) Amsler, C. D. Use of computer-assisted motion analysis for quantitative measurements of swimming behavior in peritrichously flagellated bacteria. *Anal. Biochem.* **1996**, *235*, 20−25.
(26) Gestwicki, J. E.; Strong, L. E.; Kiessling, L. L. Tuning chemotactic responses with synthetic multivalent ligands. *Chem Biol.* **2000**, *7*, 583−91.
(27) Fein, J. B.; Boily, J. F.; Yee, N.; Gorman-Lewis, D.; Turner, B. Potentiometric titrations of *Bacillus subtilis* cells and a comparison of modeling approaches. *Geochim. Cosmochim. Acta* **2005**, *69*, 1123−1132.
(28) Borrok, D.; Fein, J. B. The impact of ionic strength on the adsorption of protons, Pb, Cd, and Sr onto the surfaces of Gram-negative bacteria: testing nonelectrostatic, diffuse, and triple layer models. *J. Colloid Interface Sci.* **2005**, *286*, 110−126.
(29) Fein, J. B.; Daughney, C. J.; Yee, N.; Davis, T. A. A chemical equilibrium model for metal adsorption onto bacterial surfaces. *Geochim. Cosmochim. Acta* **1997**, *61*, 3319−3328.
(30) Fowle, D.; Fein, J. B. Experimental measurements of the reversibility of metal−bacteria adsorption reactions. *Chem. Geol.* **2000**, *168*, 27−36.
(31) De Pina, K.; Navarro, C.; McWalter, L.; Boxer, D. H.; Price, N. C.; Kelly, S. M.; Mandrand-Berthelot, M.; Wu, L. Purification and characterization of the periplasmic nickel-binding protein NikA of *Escherichia coli* K12. *Eur. J. Biochem.* **1995**, *227*, 857−865.
(32) Eitinger, T.; Mandrand-Berthelot, M. Nickel transport systems in microorganisms. *Arch. Microbiol.* **2000**, *173*, 1−9.
(33) Heddle, J.; Scott, D. J.; Unzai, S.; Park, S.; Tame, J. R. H. Crystal structures of the liganded and unliganded nickel-binding protein NikA from *Escherichia coli*. *J. Biol. Chem.* **2003**, *278*, 50322−50329.
(34) Baes, C. F.; Mesmer, R. E. *The hydrolysis of cations*. Wiley: New York, 1976.
(35) Beveridge, T. J.; Koval, S. F. Binding of metals to cell envelopes of *Escherichia coli* K-12. *Appl. Environ. Microbiol.* **1981**, *42*, 325−335.
(36) Daughney, C. J.; Siciliano, S. D.; Rencz, A. N.; Lean, D.; Fortin, D. Hg(II) adsorption by bacteria: a surface complexation model and its application to shallow acidic lakes and wetlands in Kejimkujik national park, Nova Scotia, Canada. *Environ. Sci. Technol.* **2002**, *36*, 1546−1553.
(37) Westall, J. C. FITEQL, a computer program for determination for chemical equilibrium constants from experimental data, version 2.0, Oregon State University, Corvallis, OR, 1982.
(38) Smith, R. M.; Martell, A. E. *Critical Stability Constants V. 1*; Plenum Press: New York and London, 1978.
(39) Fein, J. B.; Boily, J.; Guclu, K.; Kaulbach, E. Experimental study of humic acid adsorption onto bacteria and Al-oxide mineral surfaces. *Chem. Geol.* **1999**, *162*, 33−45.
(40) Sanchez, S. R.; Schiffrin, D. J. Bacterial chemo-attractant properties of metal ions from dissolving electrode surfaces. *J. Electroanal. Chem.* **1996**, *403*, 39−45.

(41) Jerez, C. A. Chemotactic transduction in biomining microorganisms. *Hydrometallurgy* **2001**, *59*, 347−356.
(42) Stringfellow, W. T.; Alvarez-Cohen, L. Evaluating the relationship between the sorption of PAHs to bacterial biomass and biodegradation. *Water Res.* **1999**, *33*, 2535−2544.
(43) Walsh, F.; Mitchell, R. *Inhibition of bacterial chemoreception by hydrocarbons*; LSU-SG-73-01; Center for Wetland Resources, Louisiana State University: Baton Rouge, LA, 1973; pp 275−278.
(44) Gestwicki, J. E.; Kiessling, L. L. Inter-receptor communication through arrays of bacterial chemoreceptors. *Nature* **2002**, *415*, 81−84.

Received for review November 11, 2004. Revised manuscript received May 13, 2005. Accepted May 16, 2005.

ES0482381